https://doi.org/10.30799/jnst.167.18040525 J. Nanosci. Tech. - Volume 4 Issue 5 (2018) 555–559

Share Your Innovations through JACS Directory

Journal of Nanoscience and Technology

Visit Journal at http://www.jacsdirectory.com/jnst

ISSN: 2455-0191

Visible Light Responsive Nickel and Sulphur Co-Doped TiO_2 Mesoporous Nanomaterial for the Degradation of Orange-II Dye and Antibacterial Activity on *Escherichia coli*

K.V. Divya Lakshmi, T. Siva Rao*

Department of Inorganic and Analytical Chemistry, Andhra University, Visakhapatnam – 530 003, Andhra Pradesh, India.

ARTICLE DETAILS

Article history:
Received 02 October 2018
Accepted 12 November 2018
Available online 06 December 2018

Keywords:
TiO_2
Sol-Gel Method
Orange-II
Photocatalytic Activity

ABSTRACT

Nickel and sulfur co-doped TiO_2 photocatalyst were prepared by using sol-gel method with dopants precursors of nickel nitrate and thiourea. Prepared samples were characterized by XRD, UV-Vis-DRS, TEM, BET, FT-IR and SEM-EDX. These characterization and experimental results revealed that there is a formation of anatase phase, decreased band gap 2.62 eV for NIST-2, small particle size 7.3 nm and high surface area 142.62 m^2/g. The FT-IR frequency shift for Ti-O-Ti was observed from 569 cm^{-1} to 460-560 cm^{-1} for co-doped TiO_2. The efficiency of photocatalytic and antibacterial was evaluated by degradation of Orange-II dye and *Escherichia coli* (MTCC-443) respectively. The complete degradation of Orange-II was achieved in 120 min at optimum reaction parameters for NIST-2 at pH-3, catalyst dosage-100 mg/L and initial dye concentration at 10 mg/L.

1. Introduction

The evaluation of several hazardous dyes from many textile industries in to the effluents is a major source for pollution of water bodies. These organic compounds are persistent in to the environment it can directly impact the health of ecosystems and present a threat to human beings due to the contamination of surface water and ground water sources [1]. Azo dyes are the largest group of dyes used for dyeing of cotton fibers in textile industries. They are not readily degradable and typically completely removable from water by conventional chemical wastewater treatments [2, 3]. Orange-II is widely used in dyeing of textile paper, leather, food industry, cosmetics [2] and thus found in waste water of the related industries. Orange-II mainly affects the liver and decreases the red blood corpocells. They are not readily decompose and not completely removable from waste water [4]. Polluted water contains harmful pathogenic bacteria and fungi these are contaminated in to the water sources. *Escherichia coli* (*E. coli*) is a gram –ve bacteria it causes urinary tract infections, and diarrhea. A wide range of methods has been developed for the removal of synthetic dyes from wastewaters to decrease their impact on the environment. In heterogeneous photo catalysis TiO_2 is one of the most efficient semiconductor, considerable environmental applications and it shows photocatalytic removal of dyes and certain pathogenic bacteria from waste water under UV-light irradiation, because of its strong oxidizing power, non-toxicity, long-term stability against photo and chemical corrosion, cost effective and ability to mineralize refractory organic pollutants under ambient pressure and temperature [5]. To enhance the quantum efficiency of TiO_2 in visible region there is a need to decrease a band gap and electron hole (e^+/h^-) recombination by doping of TiO_2 with metal and non-metal elements [6, 7]. In this present work we aimed to synthesize Ni and S co-doped TiO_2 using sol-gel method. Ni is preferred because it creates a new energy level above the valance band of TiO_2. It causes narrowing the band gap and active in visible light [8,9]. The doping of S replaces the lattice titania into TiO_2 matrix [10, 11]. The main advantage of sol-gel method using catalytic material having excellent control over the product properties and accessible in all key processing steps of gel, aging, drying heat treatment [12]. Hence Ni and S were selected based on the above advantages for the synthesis of co-doped TiO_2 nano material.

2. Experimental Methods

2.1 Materials

All the chemicals used in the synthesis process were reagent grade and the solutions were prepared with double distilled water without further purification. N-butyltetraorthotitanate ($Ti(OBu)_4$), manganese nitrate $[Ni(NO_3)_2].6H_2O$ and thiourea are obtained from E-Merck (Germany) were used as a precursors of titanium, nickel, sulfur for preparing undoped TiO_2 and co-doped TiO_2 catalysts respectively. Orange-II dye was used as a model dye pollutant obtained from High media, India. Ethanol and nitric acid were obtained from E-Merck (India) used as a solvent in the reaction procedure.

2.2 Preparation of Ni and S Co-Doped TiO_2

Nickel and sulfur co-doped nano titania (0.75 Wt% of Ni and 0.25 Wt % of S) was synthesized by sol-gel method. 40 mL of ethanol along with the 20 mL of n-Butylorthotitanate taken in a beaker-1 and acidified with 3.2 mL of nitric acid and continuous stirring for 30 min; this solution is considered as solution-1. 40 mL of ethanol and required weight percentage amount of dopants and 7.2 mL of water taken in a beaker-2 and continues stirring for 30 min; this solution is considered as solution-2. Then the solution-2 was added solution-1 drop wise slowly and stirred until turbidity obtained and kept the turbid solution aside for aging 48 h at room temperature to obtain a gel. Dried the gel at 70 °C in hot air oven and ground for fine crystalline powder. This powder was calcined at 450 °C for about 5 h in a muffle furnace. The same procedure was adopted for the preparation of undoped TiO_2 without addition of dopants.

2.3 Characterization of Catalyst

The crystalline structure of photocatalyst were determined by powder X-ray diffraction (XRD) spectra taken (model ultima IV Rigaku) using anode Cu-WL 1 (λ=1.5406nm) radiation with a nickel filter. The applied current and voltage were 40 mA and 40 kV respectively. The average crystallite size of anatase was determined according to the Scherrer's equation using (FWHM) data of the selected peak. The surface area and porosity measurements were carried out with a micrometrics Gemini VII surface area analyzer. FT-IR spectra of the samples were recorded on a FT-IR spectrometer (Nicolet Avatar 360). The Diffuse reflectance spectra (DRS) were recorded with a Shimadzu 3600 UV-Visible- NIR Spectrophotometer equipped with an integrating sphere diffuse reflectance accessory, using $BaSO_4$ as reference scatter. Powder samples were loaded into a quartz cell and spectra were recorded in the range of

*Corresponding Author:sivaraotvalluri.16@gmail.com(Tirukkovalluri Siva Rao)

https://doi.org/10.30799/jnst.167.18040525

Cite this Article as: K.V. Divya Lakshmi, T. Siva Rao, Visible light responsive nickel and sulphur co-doped TiO_2 mesoporous nanomaterial for the degradation of orange-II dye and antibacterial activity on *Escherichia coli*, J. Nanosci. Tech. 4(5) (2018) 555–559.

200-900 nm. The nitrogen adsorption/desorption isotherms were recorded 2-3 times to obtain reproducible results and reported by BJH surface/volume mesopore analysis. The micro pore volume was calculated using the Frenkel-Halsey-Hill isotherm equation. Each sample was degassed at 300 °C for 2 h. The size and shape of the nano particles were recorded with TEM measurements using JEOL/JEM 2100, operated at 200 kV. The morphology and elemental composition of the catalyst was characterized using scanning electron microscope (SEM) (ZEISS-SUPRA 55 VP) equipped with an energy dispersive X-ray (EDS) spectrophotometer and operated at 20 kV. The extent of Orange-II degradation was monitored using UV-Vis spectrophotometer (Shimadzu 1601).

2.4 Photo Catalytic Activity of the Catalyst-Degradation Orange-II Dye

The photocatalytic activity of the synthesized catalyst, Ni and S co-doped nano titania was carried out by degradation of Orange-II dye under visible light irradiation in the photocatalytic reactor [13]. A high pressure 400 W (35,000 lm) mercury vapour lamp with UV filter (Oriel, 51472) was used as a visible light irradiation source. The degradation procedure was performed by taking 100 mL of Orange-II dye solution of required concentration (1-10 mgL^{-1}) containing sufficient amount of the catalyst in a 150 mL Pyrex glass vessel under continuous stirring placed about 20 cm away from the light source. The running water was circulated around the sample container to filter IR radiation to maintain constant solution temperature in a pyrex glass reaction vessel. The solution was stirred in dark for 30min to attain adsorption – desorption equilibrium of Orange-II dye on the catalyst surface. After visible light illumination small aliquots of sample were collected from the reaction mixture using Millipore syringe (0.45 µm) at different intervals of time to observe the change in Orange-II dye concentration by measuring the absorbance at 487 nm using UV-visible (Milton Roy Spectronic 1201) spectrophotometer. A pH meter (Elico Digital pH meter model 111E, EI) was used for adjusting and investigation of pH variation during the degradation process. The pH of the dye solutions was adjusted prior to irradiation by addition of 0.1 N NaOH / 0.1 N HCl to get required pH [30]. The percent of degradation of Orange-II dye was calculated from the following equation.

$$\% \text{ of Degradation} = A_0 - A_t / A_0 \times 100$$

where, A_0 is initial absorbance of dye solution before degradation and A_t is absorbance of dye solution at time t.

2.5 Antibacterial Activity

Antibacterial activity study of 0.75 Wt % of Ni and 0.25 Wt % S (NIST-2) was carried out by Agar-well diffusion method [14] against bacterial strains namely and Gram negative bacteria *Escherichia coli* (MTCC-443). Nutrient Agar (High media-India) dissolved in water was distributed in 100 mL conical flask and sterilized in an autoclave at 121 °C 15 lbp for 15 min. After autoclaved the media, poured sterilized petri plates were prepared and swabbed using L-shaped glass rod with 100 µL of 24 h mature broth culture of bacterial strain. The wells were made by sterile cork-borer. Wells are created in the petri plates and different concentrations of TiO_2 co-doped (NIST-2) nano particles are injected (200 µg/mL, 300 µg/mL and 400 µg/mL). The TiO_2 nano particles were dispersed in sterile water and it was used as a negative control and simultaneously the standard Antibiotic Chloramphenicol (100 µg/mL) as positive control were tested against the bacterial pathogen, then the plates were incubated 24 h at 37 °C. In the zone of inhibition of every well measured in mm.

3. Results and Discussion

3.1 X-Ray Diffraction Studies (XRD)

The XRD pattern of Ni and S co-doped TiO_2 along with undoped TiO_2 showed in Fig. 1. From figure the diffraction peak showed that anatase phase at 2θ=25.3°. The diffraction peaks at 2θ values 25.3°, 38.3°, 48.2°, 54.7° are corresponding to planes of (100), (004), (200) and (211) respectively. This is maybe indicated that Ni and S incorporated in to TiO_2 lattice by substituting Ti and O respectively. The radius of Ni is 0.72 Å and Ti^{4+} is 0.68 Å, hence Ni can easily replace some Ti^{4+} ions in TiO_2 lattice [15] and also sulfur as S^{6+} ion which can replaces the lattice Ti^{4+} into TiO_2 matrix [16] inwhich ionic radius is 1.370 Å and oxygen ionic radius is 1.34 Å. The average crystallite size of undoped and co-doped samples were calculated using Scherrer's equation the values are given in Table.1. The average crystallite sizes of undoped and co-doped samples TiO_2 samples 13.5 and 5.5 nm. It is observed that the crystallite size decreases due to increasing the metal ion content in to TiO_2 lattice crystal strain increases grain growth decreases and hence, the particle size decreases [17].

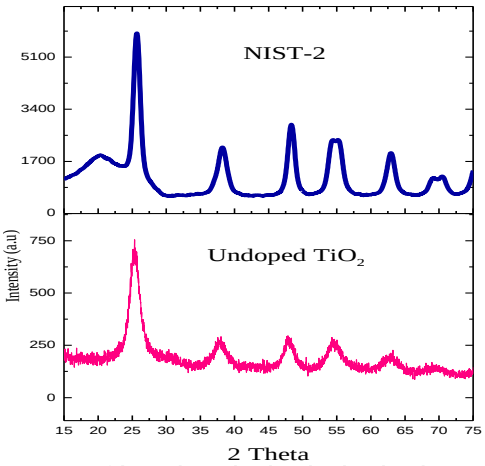

Fig. 1 The XRD pattern of the synthesized undoped and co-doped TiO_2

3.2 UV-Vis-Diffuse Reflectance Spectra (UV-Vis-DRS)

The UV-Vis-Diffuse reflectance spectra of undoped and co-doped TiO_2 are showed in Fig. 2. The co-doping of Ni and S in to TiO_2 lattice extended the strong absorption shift towards visible region. This is may be due to the Ni^{2+} and S^{6+} deflected the formation of extra energy level near the CB and VB edge and instigates a prodigious narrowing of bandgap [8]. The bandgap of the samples was calculated from reflectance spectra [F(R)] using Kubelka-Munk formalism and Tauc plot method [18] is shown in Fig. 3. The band gap values of undoped and co-doped 3.2 eV and 2.62 eV. It is observed that the co-doped sample had reduced band gap when compared to undoped TiO_2 (Table 1) and active in visible region.

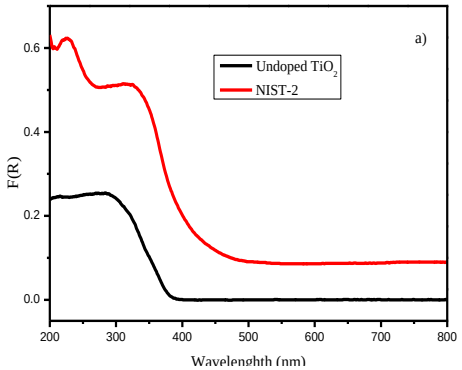

Fig. 2 The DRS spectra of undoped and co-doped (NIST-2) TiO_2

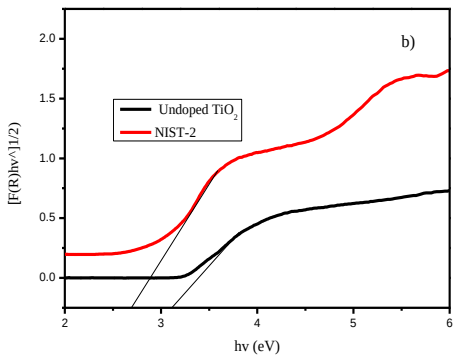

Fig. 3 Plot of transformed Kubelka-Munk $[F(R)h\nu]^2$ versus $h\nu$ for co-doped (NIST-2) and undoped TiO_2

3.3 Transmission Electron Microscopy (TEM) and Brauner-Emmitt-Teller (BET)

The TEM images of co-doped TiO_2 is showed in Fig. 4. It is indicated that the co-doped TiO_2 having less particle size with spherical shape with depicts the selected area diffraction (SAED) pattern of the NIST-2, it is clearly indicated well defined concentric rings which were due to the diffraction from the (101), (004), (200), (211) planes of the anatase TiO_2. The average particle size calculated from Gaussian fitting of size histogram (Fig. 4) [19] and found to be 7.5 nm.

https://doi.org/10.30799/jnst.167.18040525

Cite this Article as: K.V. Divya Lakshmi, T. Siva Rao, Visible light responsive nickel and sulphur co-doped TiO_2 mesoporous nanomaterial for the degradation of orange-II dye and antibacterial activity on *Escherichia coli*, J. Nanosci. Tech. 4(5) (2018) 555–559.

The BET surface area of synthesized catalysts of undoped and co-doped (NST-2) TiO_2 nano catalysts are 76.368 m^2/g and 142.156 m^2/g. The pore size and volumes are given in Table 1. These results confirmed that NIST-2 showed high surface area compared to undoped TiO_2.

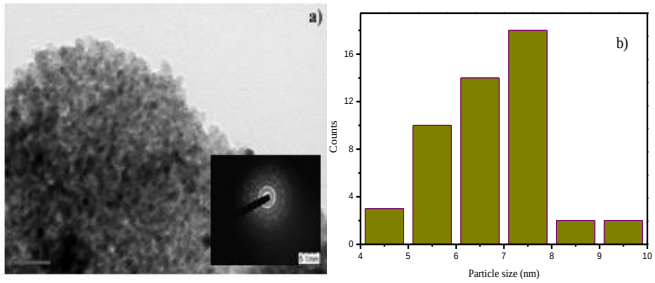

Fig. 4 The TEM images of a) co-doped TiO_2 b) size histogram and Gaussian fitting of NIST-2

Table 1 Crystallite size (XRD), band gap (UV-VIS- DRS) and BET surface area

S.No	Catalyst	Crystallite size (nm)	Band gap Energy (eV)	BET surface area analysis		
				Surface area (m^2/g)	Pore Volume (cm^3/g)	Pore Size (nm)
1	NIST-2	5.5	2.62	142.156	0.223	5.7
2	Undoped TiO_2	13.3	3.2	76.3687	0.2153	10.3

3.4 Fourier Transform –Infra Red Spectroscopy (FT-IR)

The FT-IR spectra for undoped and co-doped (NIST-2) TiO_2 were presented in Fig. 5. The stretching vibrations of OH belongs to Ti-OH on the surface and bending vibrations of adsorbed H-OH molecule are appeared at 3012 cm^{-1}, 3464 cm^{-1}, 1620 cm^{-1} and 1635 cm^{-1} [21]. The stretching vibrations of Ti-O-Ti band in undoped TiO_2 located at 569 cm^{-1}. After co-doping of Ni and S in to TiO_2 lattice the stretching vibrations of skeletal Ti-O-Ti shifted to 460 cm^{-1}, 560 cm^{-1} and 1064 cm^{-1} [22, 17] indicated that Ni and S co-doped in to TiO_2 lattice by substituting Ti and O respectively.

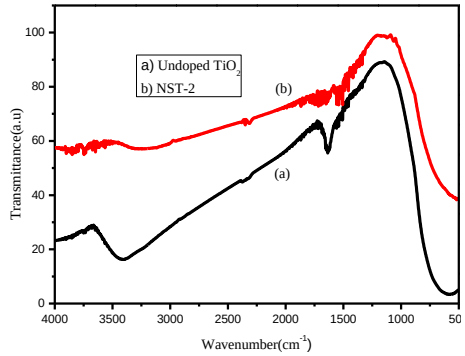

Fig. 5 a) FT-IR spectrum of undoped TiO_2 and b) co-doped TiO_2

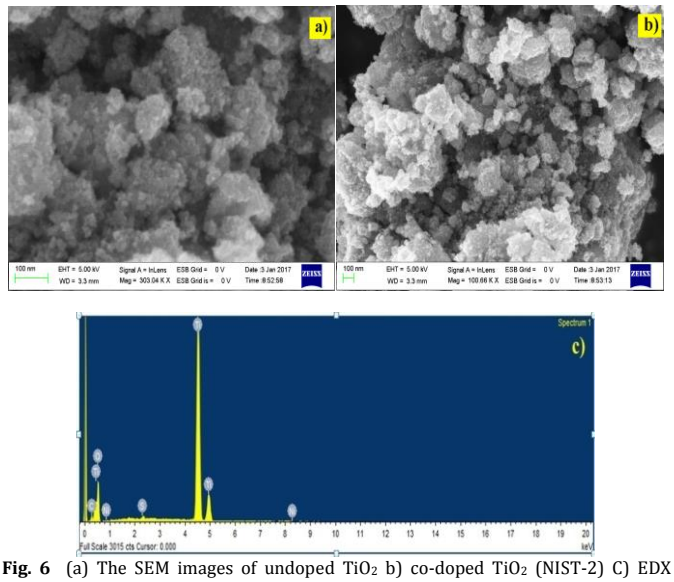

Fig. 6 (a) The SEM images of undoped TiO_2 b) co-doped TiO_2 (NIST-2) C) EDX spectrum of co-doped TiO_2

3.5 Scanning Electron Microscopy and Energy Dispersive X-Ray Photo Electron Spectroscopy (SEM-EDX)

The surface morphology of synthesized co-doped TiO_2 (NIST-2) nano particles have been investigated by SEM and EDS. The results are given in Fig. 6. From the figures indicated that the samples exhibited small particles with agglomerated and spherical shape with smooth morphology. The EDX spectrum (Fig. 6c) NIST-2 indicated that the constituent elements are present in the catalysts samples. It is concluded that Ni and S are successfully incorporated in to TiO_2 lattice.

3.6 Evaluation of Photocatalytic Activity of Ni and S Co-Doped TiO_2 by Degradation of Orange –II under Visible Light

The optimum reaction conditions are attained by varying the reaction parameters, such as dopant concentration, effect of pH, catalyst dosage and initial dye concentration. The rate of degradation of orange II formed during the reaction course was calculated by multiplying the slope of each curve with 2.303.

3.6.1 Effect of Dopant Concentration on the Degradation of Orange II

The rate of degradation of orange II has been quantified by the measurement of orange II absorbance and the results are presented in Fig. 7. It can be observed that the photocatalytic performance of TiO_2 was higher for all co-doped TiO_2 photocatalysts than undoped TiO_2. But, NIST-2 co-doped TiO_2 shown highest percentage degradation under visible light irradiation. The result shows that the rate of degradation is higher in (NIST-2) than that of other catalysts. This is may be due to the dopant concentration increases particle size decreases and surface area increases leads to higher rate of photocatalytic degradation.

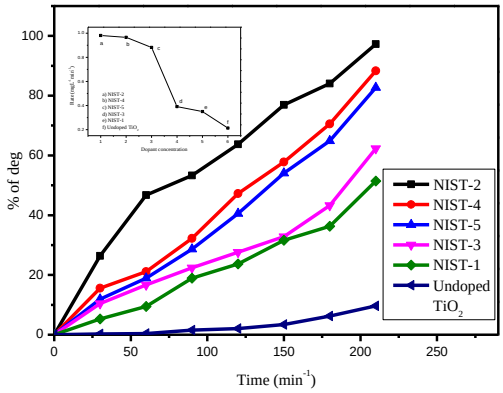

Fig. 7 Effect of dopant concentration on degradation of orange II, pH of 3, catalyst dosage of 100 mg/L

3.6.2 Effect of pH

The sample exhibiting best photocatalytic performance (NIST-2) was selected as further experiments were conducted with it. To find out the optimum pH at constant dye concentration (10 mg/L) and catalyst weight (100 mg/L) experiments were done at different pH values. The experiment results given in Fig. 8 and the rate of degradation depicted in figure.

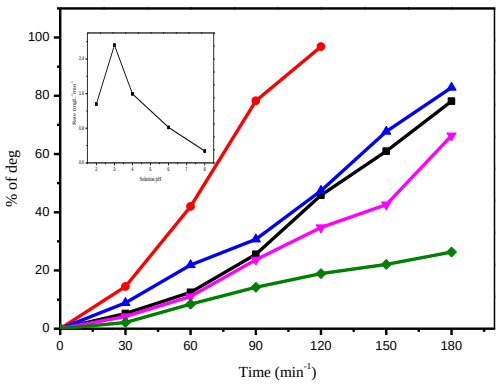

Fig. 8 The effect of pH on degradation of orange II, catalyst dosage of 100 mg/L

From the results indicated that at pH-3 the rate of degradation is very high. This is may be interpreted that at low pH positive holes acts as the major oxidant species. Hence, at acidic pH the adsorption process was favoured by the electrostatic attraction between the positively charged

https://doi.org/10.30799/jnst.167.18040525

Cite this Article as: K.V. Divya Lakshmi, T. Siva Rao, Visible light responsive nickel and sulphur co-doped TiO_2 mesoporous nanomaterial for the degradation of orange-II dye and antibacterial activity on *Escherichia coli*, J. Nanosci. Tech. 4(5) (2018) 555–559.

surface of the catalyst and dye molecules [22]. Further increasing the pH value the rate of degradation decreases due to columbic repulsion between the catalyst and dye molecules it causes decrease the rate of degradation would enhance degradation percentage and it reaches a maximum at pH 3.

3.6.3 Effect of Catalyst Dosage

Experiments were carried out to achieve an optimum catalyst dosage by varying the amount of the selected co-doped photocatalyst from 50 mg/L to 200 mg/L other parameters kept constant. The effect of the co-doped photocatalyst dose on percentage degradation of orange II with respect to time can be observed from Fig. 9. The percentage of degradation of increases with increase of photocatalyst loading up to 100 mg/L and then decreases. The increased amount of photcatalyst increases the quantity of absorption of photons increases the degradation rate increases The concentration is higher than 100 mg/L, catalysts, by collision between active molecules and ground state molecules of co-doped TiO_2 and also turbidity of the solution increases as concentration increases this restricts the penetration of light for activating the deactivated particles of co-doped TiO_2 [23]. This causes the decreases in rate of degradation of orange-II dye.

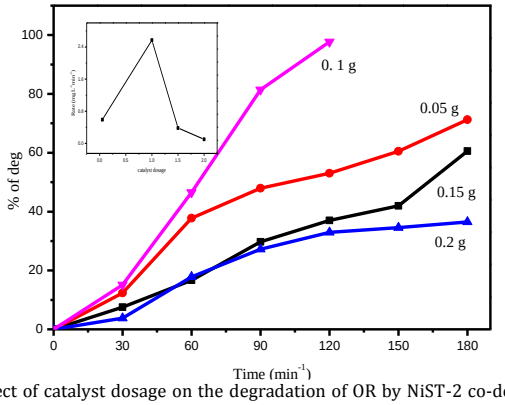

Fig. 9 Effect of catalyst dosage on the degradation of OR by NiST-2 co-doped TiO_2 here pH-3 and OR = 10 mg/L

3.6.4 Effect of Initial Dye Concentration

The role of initial concentration of a dye on the degradation rate was carried out at constant catalyst dose (100 mg/L) and at pH-3. The degradation rate values and percentage rate degradation has been presented in Fig. 10. Here the influence of initial concentration of a dye on the rate of degradation was studied with different concentration (5 mg/L – 20 mg/L) of orange II dye solution at a fixed dosage of selected co-doped photocatalyst using a pH of solution 3. The photocatalytic degradation increases with an increase in the concentration of dye up to 10 mg/L. Because, as the concentration of the dye increase, more dye molecules will be available for excitation and energy transfer. But beyond the optimum concentrations, the dye molecules starts covering the surface of photocatalyst from light intensity [24]. Hence, there is a decrease in photocatalytic activity beyond the 10 mg/L dye concentration.

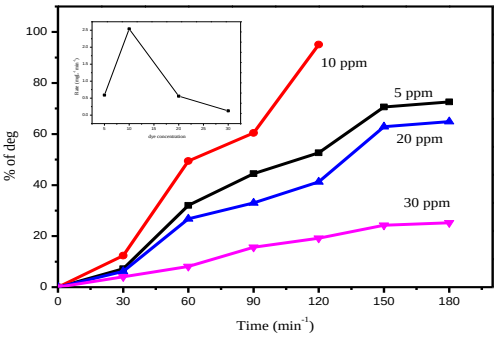

Fig. 10 Effect of initial concentration of the dye on the rate of degradation of dye (pH = 3 and catalyst dosage- 100 mg/L)

3.7 Antibacterial Studies

The antibacterial activity of TiO_2 nano particles were carried out by agar-well diffusion method against *Escherichia coli* (MTCC-443) and different concentration of co-doped TiO_2 (NIST-2) nano particles were taken in different wells in a petri dish with a concentration ranging from 200 µg/mL, 300 µg/mL, 400 µg/mL and chloromphenicol (control). The anti-bacterial petri plates are showed in Fig. 11. The bacterial growth of zone diameter was determined and presented in Table 2. The activity results were showed that (400 µg/mL) is best concentration for the co-doped TiO_2 for the zone of inhibition of both the bacteria and also very nearer to the standard values, therefore the co-doped TiO_2 nano particles exhibiting better antibacterial activity. This inhibition may be due to the electron hole which is forms in valance band of TiO_2 by irradiation of catalyst with visible light. During the visible light this e^-/h^+ +ve hole acts as a strong oxidizing agent could degrade the protein coat of the bacteria leads to the inhibition of the growth of the organism.

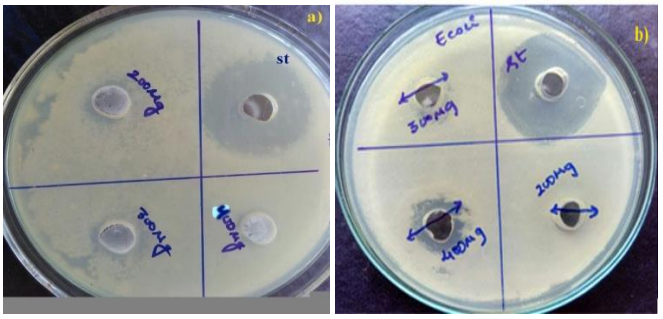

Fig. 11 Zone of inhibition of a) Undoped TiO_2 b) co-doped (NIST-2) TiO_2

Table 2 The zone of inhibition of co-doped TiO_2 nano particles (NIST-2) against *Escherichia coli* (MTCC-443)

S. No.	Catalyst	200 µg/mL	300 µg/mL	400 µg/mL	Standard 100 µg/mL (Chloramphenicol)
1	NIST-2	10.3	12.2	15.2	15.2
2	Undoped TiO_2	-	-	-	23.1

4. Conclusion

Ni and S co-doped TiO_2 were successfully synthesized by sol-gel method. The synthesized catalysts characterised by various analytical techniques. All the co-doped samples showed anatase phase. The doping of Ni inhibits the electron/hole recombination and acts as charge carrier during photocatalytic degradation under visible light irradiation. Sulfur causes the shift in absorbance band of TiO_2 from UV to visible region. 0.75 wt% Ni and 0.25 wt% S co-doped TiO_2 exhibited small particle size, high surface area gives high photoctalytic activity compared to undoped TiO_2. Finally the optimum reaction parameters were established and Orange-II dye (10 mg/L) was successfully degraded by 100 mg/L co-doped catalyst (NIST-2) at pH-3 in 120 min and also NIST-2 showed strong antibacterial activity against *Escherichia coli* (MTCC-443). It may be concluded that NIST-2 co-doped TiO_2 acts as better photocatalytic activity and good antibacterial agent.

Acknowledgements

Prof. T. Siva Rao acknowledges to SE/EMEQ-400/2014 project for the financial assistance to carryout research work. K.V. Divya Lakshmi thankful to the University Grants Commission (UGC) for providing BSR fellowship.

References

[1] M.A. Ahmed, Emad E. El-Katori, Zarha, H. Gharni, Photocatalytic degradation of methylene blue dye using Fe_2O_3/TiO_2 nanoparticles prepared by sol–gel method, Jour. Alloy. Compd. 553 (2013) 19-29.
[2] K. Hunger, Industrial dyes: Chemistry, properties, applications, Wiley-VCH, Weinheim, 2003.
[3] M.H. Habibi, M.N. Esfahani, T.A. Egerton, Preparation, characterization and photocatalytic activity of TiO_2/methylcellulose nanocomposite films derived from nanopowder TiO_2 and modified sol–gel titania, J. Mater. Sci. 42 (2007) 6027-6035.
[4] L.C. Marija, M. Nedeljko, R. Maja, S. Zoran, R. Marija, K. Melina, Photocatalytic degradation of C.I. acid orange 7 by TiO_2 nanoparticles immobilized onto/into chitosan-based hydrogel, Polym. Comp. 35 (2014) 806-815.
[5] K. Song, J. Zhou, J. Bao, Y. Feng, Photocatalytic activity of (copper, nitrogen)-codoped titanium dioxide nanoparticles, J. Am. Ceram. Soc. 91 (2008) 1369-1371
[6] Y.N.T.C. Wong. A.R. Mohamed, An overview on the photocatalytic activity of nano-doped-TiO_2 in the degradation of organic pollutants, ISRN Mater. Sci. 2011 (2011) 1-18.

https://doi.org/10.30799/jnst.167.18040525

Cite this Article as: K.V. Divya Lakshmi, T. Siva Rao, Visible light responsive nickel and sulphur co-doped TiO_2 mesoporous nanomaterial for the degradation of orange-II dye and antibacterial activity on *Escherichia coli*, J. Nanosci. Tech. 4(5) (2018) 555–559.

[7] D. Dvoranova, V. Brezova, M. Mazur, and M. A. Malati, Investigations of meta-doped titanium dioxide photocatalysis, Appl. Catal. B: Environ. 37 (2002) 91-105.
[8] H. Zhang, Z. Xing, Y. Zhang, Z. Li, X. Wu, C. Liu, Q. Zhu, W. Zhou, Ni^{2+} and Ti^{3+} co-doped porous black anatase TiO_2 with unprecedented-high visible-light-driven photocatalytic degradation performance, RSC Adv. 5 (2015) 107150-107157.
[9] Prasetyo Hermawan, Harno Dwi Pranowo, Indriana Kartini, Physical Characterization of Ni(II) doped TiO_2 nanocrystal by sol-gel process, Indo. J. Chem. 11 (2011) 135-139.
[10] L. Shao-You, T. Qun-Li, F. Qing-Ge, Synthesis of S/Cr doped mesoporous TiO_2 with high-active visible light degradation property via solid state reaction route, Appl. Surf. Sci. 257 (2011) 5544-5551.
[11] D.J. Wu. X.J. Liu, Optical investigation on sulfur-doping effects in titanium dioxide nano particles, Appl. Phys. A 97 (2009) 243-248.
[12] P. Singla, O.P. Pandey, K. Singh, Study of photocatalytic degradation of environmentally harmful phthalate esters using Ni-doped TiO_2 nanoparticles, Int. J. Environ. Sci. Tech. 13 (2016) 849-856.
[13] K. Karthik, S. Dhanuskodi, C. Gobinath, S. Prabukumar, S. Sivaramakrishnan, Photocatalytic and antibacterial activities of hydrothermally prepared CdO nanoparticles, J. Mater. Sci. Mater. Electron. 28 (2017) 11420-11429.
[14] M.H. Salama, N. Marraiki, Antimicrobial activity and phytochemical analyses of *Polygonum aviculare* L. (Polygonaceae), naturally growing in Egypt, Saudi. J. Bio. Sci. 17 (2015) 57-63.
[15] M. Hemraj Yadav, V. Sachin Otari, A. Raghvendra Bohara, S. Sawanta Mali, H. Shivaji Pawar, D. Sagar Delekar, Synthesis and visible light photocatalytic antibacterial activity of nickel-doped TiO_2 nanoparticles against Gram-positive and Gram-negative bacteria, J. Photochem. Photobiol. A: Chem. 294 (2014) 130-136.
[16] N. Sang-Hun, T. Kwan Kimb, B. Jin-Hyo, Physical property and photo-catalytic activity of sulfur doped TiO_2 catalysts responding to visible light, Catal. Today 185 (2012) 259-262.
[17] Q.R. Deng, X.H. Xia, M.L. Guo, Y. Gao, G. Shao, Mn-doped TiO_2 nano powders with remarkable visible light photocatalytic activity, Material. Lett. 65 (2011) 2051-2054.
[18] S. Chang, H. Chien-Yao, L. Pin-Han, Chang-Tuan, Preparation of phosphated Zr-doped TiO_2 exhibiting high photocatalytic activity through calcination of ligand-capped nanocrystals, Appl. catal B: Environ. 90 (2009) 233 -241.
[19] E. Gharibshahi, E. Saion, Influence of dose on particle size and optical properties of colloidal platinum nanoparticles, Int. J. Mol. Sci. 13(11) (2012) 14723-14741.
[20] N. Sharotri, D. Sud, Ultrasound-assisted synthesis and characterization of visible light responsive nitrogen-doped TiO_2 nanomaterials for removal of 2-chlorophenol, Desalin. Water. Treat. 57 (2015) 8776-8788.
[21] L. Gomathi Devi, K. Nagaraju , B. Narasimha Murthy, S. Girish Kumar, Enhanced photocatalytic activity of transition metal Mn^{2+}, Ni^{2+} and Zn^{2+} doped polycrystalline titania for the degradation of aniline blue under UV/ solar light. J. Molecul. Catal. A: Chem. 328 (2010) 44-52
[22] M.A. Rauf, S. Salman Ashraf, Fundamental principles and application of heterogeneous photocatalytic degradation of dyes in solution, Chem. Eng. Jour. 151 (2009) 10-18.
[23] E. Kusvuran, O. Gulnaz, S. Irmak, O.M. Atanur, H.I. Yavuz, O. Erbatur, Comparison of several advanced oxidation processes for the decolourization of Reactive Red 120 azo dye in aqueous solution, J. Hazard. Mater. B 109 (2004) 85-93.
[24] C.H. Chiou, R.S. Juang, Photocatalytic degradation of phenol in aqueous solutions by Pr-doped TiO_2 nano particles, J. Hazard. Mater. 149 (2007) 669-678.

https://doi.org/10.30799/jnst.167.18040525

Cite this Article as: K.V. Divya Lakshmi, T. Siva Rao, Visible light responsive nickel and sulphur co-doped TiO_2 mesoporous nanomaterial for the degradation of orange-II dye and antibacterial activity on *Escherichia coli*, J. Nanosci. Tech. 4(5) (2018) 555–559.